

Microstructure and giant magnetoresistance of FeCo–Cu nanogranular films

Changzheng Wang · Yiqing Zhang · Xiaoguang Xiao ·
Yonghua Rong · H. Y. Tsu

Received: 20 September 2006 / Accepted: 8 December 2006 / Published online: 18 May 2007
© Springer Science+Business Media, LLC 2007

Abstract A series of $(\text{Fe}_{50}\text{Co}_{50})_x\text{Cu}_{1-x}$ granular films were prepared using a magnetron controlled sputtering system. The microstructure and giant magnetoresistance (GMR) of FeCo–Cu films deposited at room temperature and then annealed at various temperatures were investigated through transmission electron microscope and conventional four probes method under room temperature, respectively. The results revealed that all FeCo–Cu films consisted of fine FeCo granules uniformly dispersed in the Cu matrix and formed fcc structure. By a non-linear least-squares method, the size distribution of FeCo granules in all as-deposited films satisfied a log-normal function. Upon varying the magnetic volume fraction (x), the GMR of as-deposited FeCo–Cu films reached a maximum of about 0.7% at the volume fraction of 31% FeCo, corresponding to the fact that the GMR has a non-monotonic relationship with the granule size. With increasing the annealing temperature, the GMR of films with lower volume fraction reached a peak at higher temperature, while for films with higher volume fraction the GMR reached a peak at lower temperature. In addition, the relationships between the full width at half maximum (FWHM) or the sensitivity of the GMR and the volume fraction were discussed in detail.

Introduction

Since the first discovery of giant magnetoresistance (GMR) effect in Co–Cu granular films by Xiao et al. [1] and Berkowicz et al. [2] simultaneously, the granular films with GMR effect has been extensively studied [3–6] due to complicated mechanisms and potential application in information industry. It is known that the GMR effect in granular films originates from the spin-dependent scattering of conduction electrons at the interface between the ferromagnetic granules and non-magnetic matrix as well as within the ferromagnetic granules, and then has a close relationship with granule size. According to Cullity's classification [7] all magnetic granules in granular films can be divided into three categories: superparamagnetic, single domain ferromagnetic and multi-domain ferromagnetic granules. They can display different magnetic property under applied fields, giving rise to different effects on the spin-dependent scattering related to GMR effect. Some experiments and theories [8–10] indicated that superparamagnetic granules play a key role in GMR effect since the smaller the granule size, the larger the ratio of surface to volume, resulting in the stronger spin-dependent scattering of conduction electrons. Meanwhile, the smaller the granule size, the easier the granules show superparamagnetic nature, hence GMR effect increases monotonically with decreasing granule size. However Sang et al. [11] found that there is no monotonic relationship between granule size and GMR effect and there exists a peak value at a certain size for a given annealing temperature, which was also proven theoretically by Gu et al. [12]. This phenomenon contradicted with above viewpoint and indicated that single domain ferromagnetic granules, rather than superparamagnetic granule, predominate in GMR effect since the fraction of single domain ferromagnetic granules and

C. Wang (✉)
Laboratory of Advanced Materials, Department of Materials
Science and Engineering, Tsinghua University, Beijing 100084,
P.R.China
e-mail: wcz@mail.tsinghua.edu.cn

C. Wang · Y. Zhang · X. Xiao
Department of Physics, Liaocheng University, Liaocheng city
252059, Shandong Province, P.R.China

Y. Rong · H. Y. Tsu
School of Materials Science and Engineering, Shanghai Jiaotong
University, Shanghai 200030, P.R.China

GMR effect has identical changing tendency with annealing temperature. In addition, Chen Xu et al. [13] confirmed that single domain ferromagnetic granules play a key role in GMR effect based on effective medium theory. Besides, Hütten et al. [14] found that when magnetic granules in granular films form multi-domain structure, their GMR effect will lose like bulk magnetic granules. To ascertain this discrepancy, we use FeCo–Cu granular films system as an example to study the relationship between granule size and GMR effect and then to reveal the effect of granule size on GMR effect in detail.

Experimental procedure

In our experiments, all $(\text{Fe}_{50}\text{Co}_{50})_x\text{Cu}_{1-x}$ granular films were sputtered respectively on glass and KCl substrate at room temperature (RT) with a spc350 multi-target magnetron controlled sputtering system. FeCo target (the weight ratio of Fe and Co is 1:1) and Cu target (99.99% purity) were separately installed on two independently controlled R.F. cathodes, and were alternatively employed to sputter these films with 30 circles of substrate per minute. The volume fraction of FeCo in the FeCo–Cu films was controlled by changing the sputtering power of FeCo target and was determined by means of energy dispersive spectrum attached to scanning electron microscope. That is to say that we first obtained the atomic ratio of Fe, Co, and Cu by means of energy dispersive spectrum attached to scanning electron microscope. And then we can calculate the volume fraction of FeCo magnetic granules, x_v , through following formula:

$$x_v = \frac{\frac{N \times x_{\text{Fe}}}{N_0} \times M_{\text{Fe}}}{\rho_{\text{Fe}}} + \frac{\frac{N \times x_{\text{Co}}}{N_0} \times M_{\text{Co}}}{\rho_{\text{Co}}} + \frac{\frac{N \times x_{\text{Cu}}}{N_0} \times M_{\text{Cu}}}{\rho_{\text{Cu}}}$$

where N is assumed to be the number of total atoms in films and N_0 is Avogadro constant ($=6.02 \times 10^{23}$). x_i stands for the atomic ratio of i atom occupying the total atoms in films. Meanwhile, M_i and ρ_i represent the molar mass and the density of i atom, respectively.

Meanwhile, the sputtering gas (Ar) pressure was 1.7×10^{-1} Pa. The film specimens for TEM observation were obtained by putting a sputtered substrate into de-ionized water with a little acetone, then by using a copper grid to hold the film floating on the water after the dissolution of the KCl substrate. TEM observations were carried out on JEM-100CX. The GMR effect were measured with conventional four probes method under room temperature and the applied fields is swept from about -1.25 T to 1.25 T. All the samples were sealed in glass tubes filled with Ar atmosphere and annealed with different temperature.

Results and discussion

Microstructure

Since the intricate structure of granular FeCo–Cu films only exists on the nanometer scale and plays a key role in GMR, it is imperative to study the nanoparticles morphology of these films through TEM observation in order to understand GMR comprehensively. Figure 1 shows Bright-field TEM micrographs of as-deposited films with various volume fraction of FeCo, respectively. It is apparent that the FeCo granules surrounded by Cu matrix are equiaxial in shape and their size in diameter is about from 1 nm to 15 nm in all as-deposited films, which indicates that these films consist of very fine FeCo granules uniformly dispersed in the Cu matrix. Meanwhile, it can be found that the granule size increase monotonically with increasing the volume fraction of FeCo granule. According to granule size, all granules can be divided into superparamagnetic, single domain ferromagnetic and multi-domain ferromagnetic granules by two critical size $D_1(T)$ and $D_2(T)$ [7, 15], where $D_1(T)$ is a critical size between superparamagnetic granules and single domain ones and $D_2(T)$ is a critical size between single domain granules and multi-domain ones. All above three kinds of granules have different magnetic properties under an applied field and thus make different contributions to the GMR effect, thus leading to the fact that GMR effect changes with the fraction of various magnetic granules. However, the fraction of various magnetic granules depends not only on the granule size but also on the size distribution significantly. Therefore, determining the size distribution is important to optimize the GMR effect.

In order to obtain the size distribution of FeCo granules, we observe the central dark-field (CDF) images of FeCo (110) reflection. Figure 2 shows electron diffraction pattern for as-deposited FeCo–Cu films with various volume fraction. It is clear that all the films show diffraction rings corresponding to Cu (111), Cu (200), Cu (220) and Cu (310), indicating that all as-deposited films form fcc structure. In addition, when the volume fraction is low, no additional diffraction rings corresponding to FeCo phase are observed except FeCo (110) diffraction rings overlapping with Cu (111). While for films with higher volume fraction, there occurred FeCo (200) diffraction rings besides FeCo (110) diffraction rings overlapping with Cu (111), indicating the coalescence of FeCo granules. Figure 3 shows the dark-field image corresponding to the operative reflection of FeCo (110), from which it can be found that FeCo granules embedded in Cu matrix are almost equiaxial in shape and their size in diameter is about from 1 nm to 15 nm, indicating that this

Fig. 1 Bright-field TEM micrograph for as-deposited FeCo–Cu films (a) 13%vol., (b) 25%vol, (c) 31%vol., (d) 41%vol.

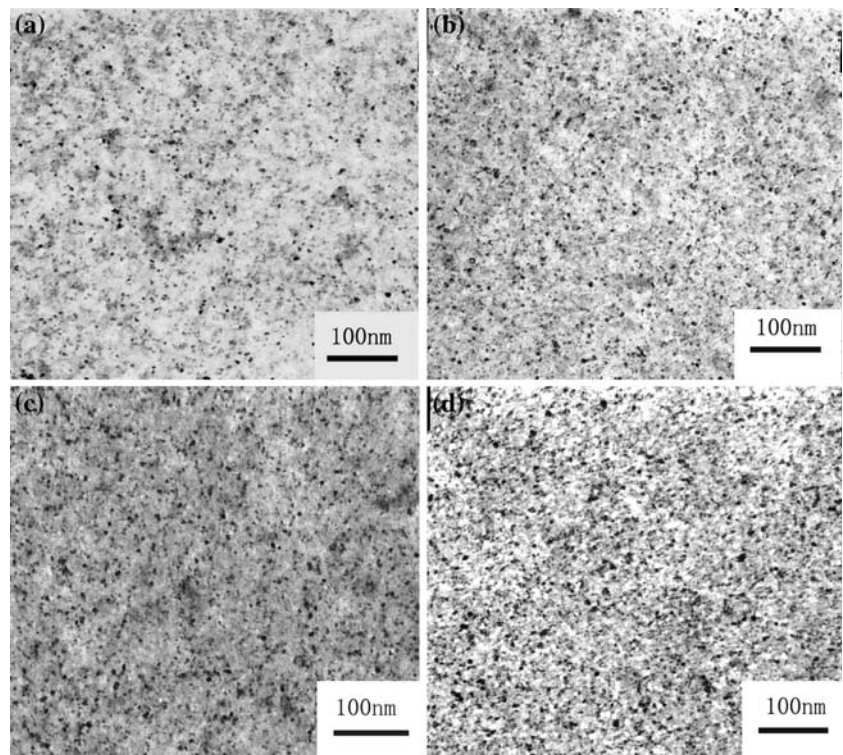
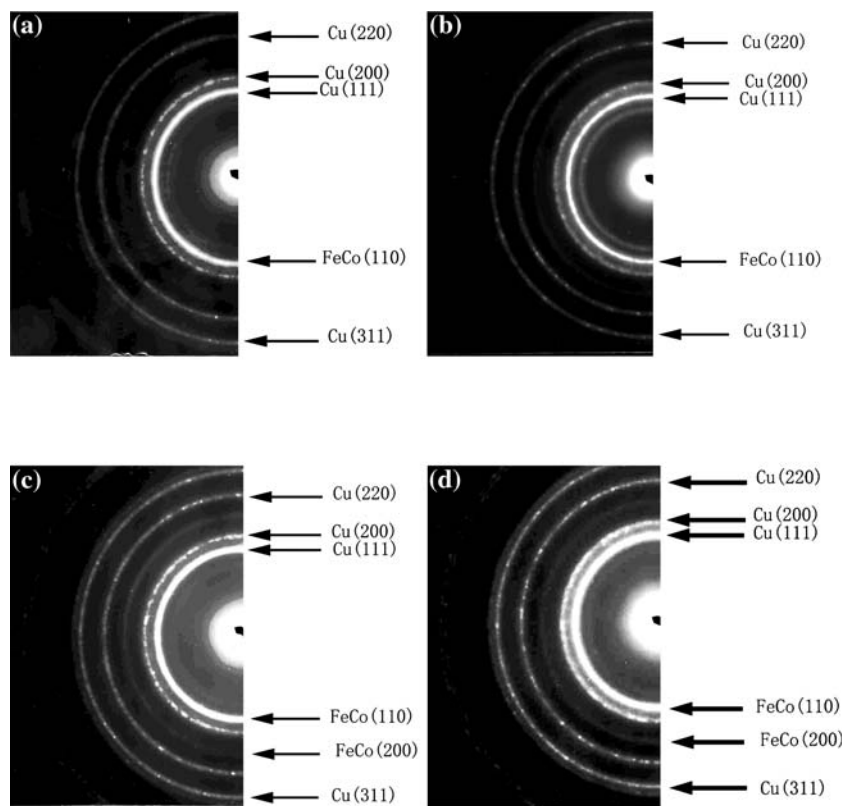


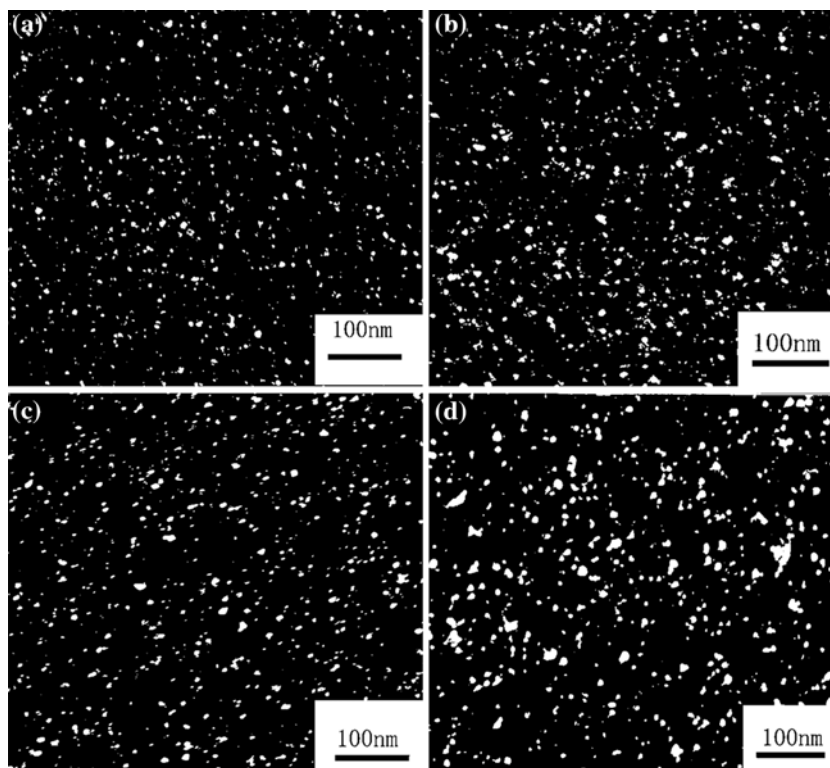
Fig. 2 Electron diffraction pattern for as-deposited FeCo–Cu films (a) 13%vol., (b) 25%vol, (c) 31%vol., (d) 41%vol.



film consist of ultrafine FeCo granules uniformly dispersed in the Cu matrix and the result is also in agreement with the bright-field micrograph mentioned above.

According to the central dark-field images of the FeCo (110) reflection we can obtain the size distribution of FeCo granules for all FeCo–Cu films.

Fig. 3 Dark-field micrograph for as-deposited FeCo–Cu films (a) 13%vol., (b) 25%vol., (c) 31%vol., (d) 41%vol.



Parent et al. [16] believed that the size distribution of granules satisfied a Gauss function. However, most researchers [17, 18] used the log-normal distribution function to describe the size distribution of magnetic granules, which has formula as follows:

$$f(D) = A \frac{1}{\sqrt{2\pi}\sigma} \exp \left\{ -\frac{[\ln(D/D_0)]^2}{2\sigma^2} \right\}$$

where σ is the variance of size distribution, D_0 is the average size of granules, A is normalization constant of the size distribution function. If the size distribution of FeCo granules satisfies a log-normal function, we can calculate the fraction of superparamagnetic, single domain ferromagnetic and multi-domain ferromagnetic granules, respectively, by the following integral:

$$x_1 = \int_0^{D_1(T)} f(D)dD, \quad x_2 = \int_{D_1(T)}^{D_2(T)} f(D)dD, \quad x_3 = \int_{D_2(T)}^{\infty} f(D)dD,$$

where x_1 , x_2 , x_3 stand for the fraction of superparamagnetic, single domain ferromagnetic and multi-domain ferromagnetic granules, respectively, and they satisfy $x_1 + x_2 + x_3 = 1$. Therefore the size distribution determines the fraction of the three kinds of granules and thus has an important effect on GMR effect.

Based on the central dark-field images in Fig. 3, the size distribution patterns for as-deposited FeCo–Cu films with various volume fractions are given by image analysis instrument, as shown in Fig. 4. It can be seen that the size distribution tends to have a tail toward larger granule size. Using the log-normal function to make a fitting for the size distribution by a non-linear least-squares method, one can see that the size distribution of FeCo granules satisfies the log-normal distribution function except an apparent error occurs in the vicinity of smaller size (<2 nm). This maybe attributed to the fact that for films with low volume fraction there are too many smaller granules, thus resulting in an error in the vicinity of smaller size. While for films with high volume fraction, the error can be decreased since the large granules predominate in films (see Fig. 4(d)). In addition, one can approximately obtain the average size of FeCo granules in various as-deposited films through fitting, as listed in Table 1. It can be seen that granule size increases with increasing the volume fraction of FeCo granules, which confirms TEM observation.

As well known, annealing temperature has an important effect on the microstructure and then on the GMR, therefore, it is imperative to study the microstructure of annealed films in order to disclose the relationship of microstructure and GMR. Figures 5 and 6 show the Bright-field TEM micrograph and dark-field micrograph for FeCo (31%vol)–Cu films annealed at 373 K and 473 K, respectively. It is clear

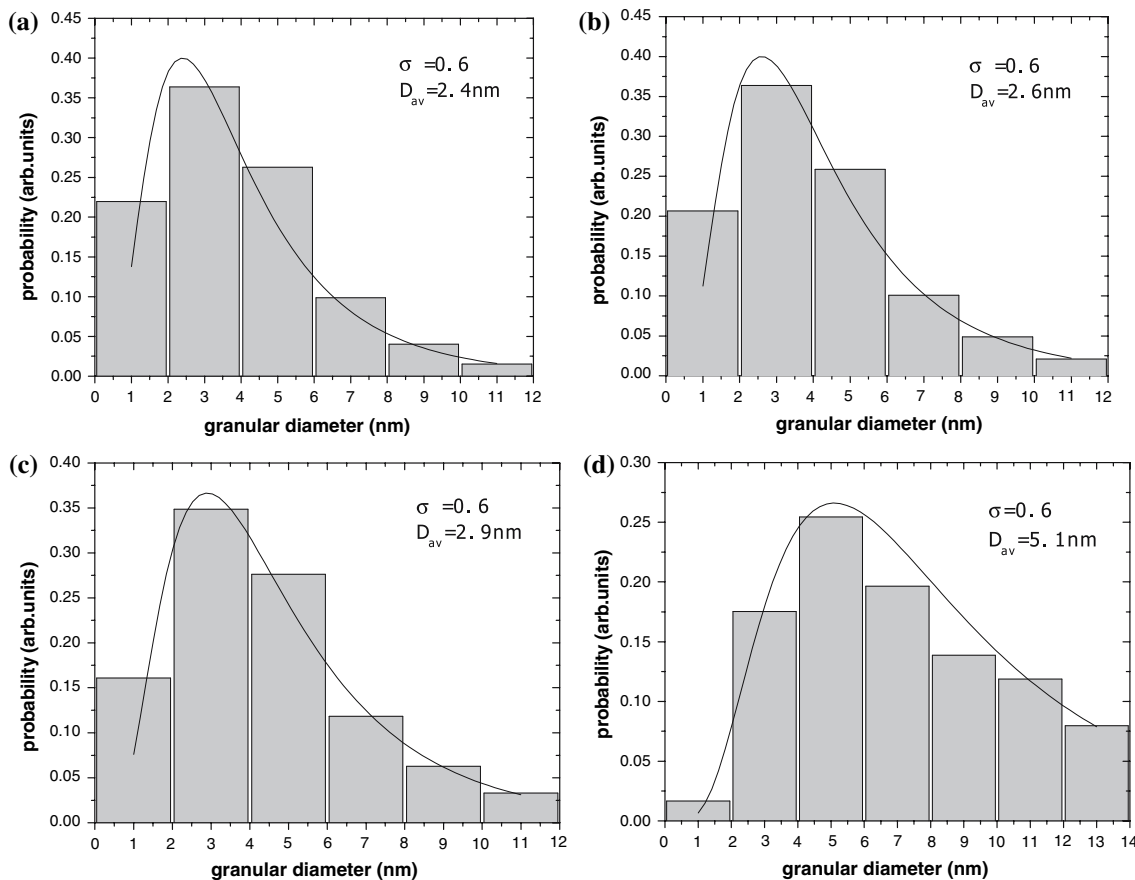


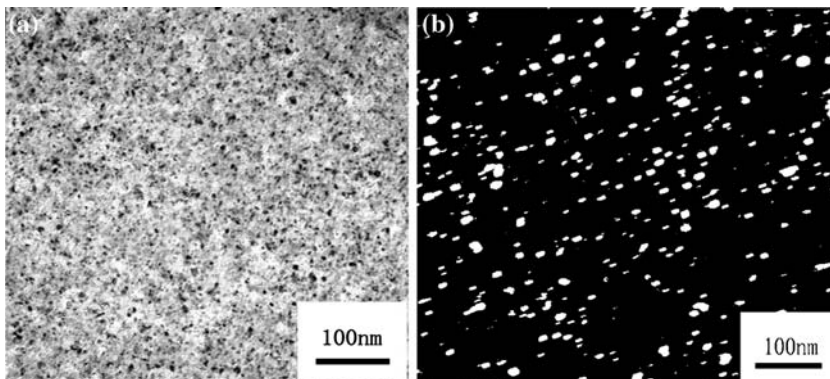
Fig. 4 The size distribution for as-deposited FeCo–Cu films (a) 13%vol., (b) 25%vol., (c) 31%vol., (d) 41%vol. The solid line is fitting lines

Table 1 The average grain size of as-deposited FeCo–Cu films with various volume fraction

Volume fraction	0.13	0.25	0.31	0.36	0.41
D_0 (nm)	2.1	2.6	2.9	3.8	5.1

that magnetic granules size increase monotonically with increasing the annealing temperature by comparing it to as-deposited films.

Fig. 5 (a) Bright-field TEM micrograph and (b) dark-field micrograph for FeCo (31%vol.)–Cu films annealed at 373 K



Magnetoresistance

Figure 7 shows the changes of resistivity without applied fields ($\rho(0)$), magnetic resistivity ($\rho_m \approx \rho(0) - \rho(1.25T)$) and GMR effect with the volume fraction at room temperature. The GMR data are presented in fraction of $GMR = [\rho(0) - \rho(H)]/\rho(0)$, where H is about the maximum field 1.25 T. It can be seen from Fig. 7(a) that $\rho(0)$ has a non-monotonic relationship with volume fraction, which is in agreement with Co–Ag and Co–Cu systems

Fig. 6 (a) Bright-field TEM micrograph and (b) dark-field micrograph for FeCo (31% vol.)–Cu films annealed at 473 K

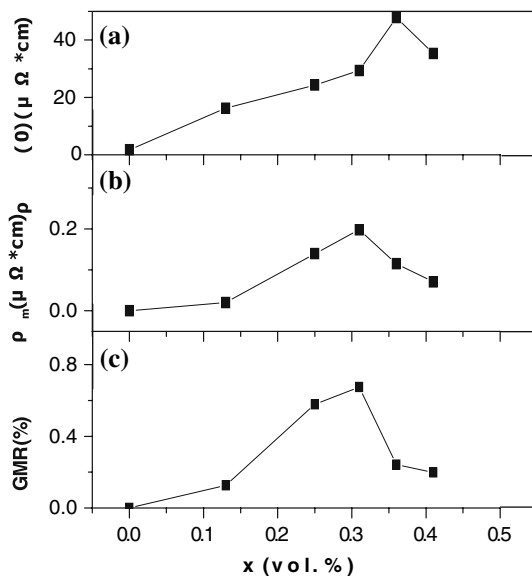
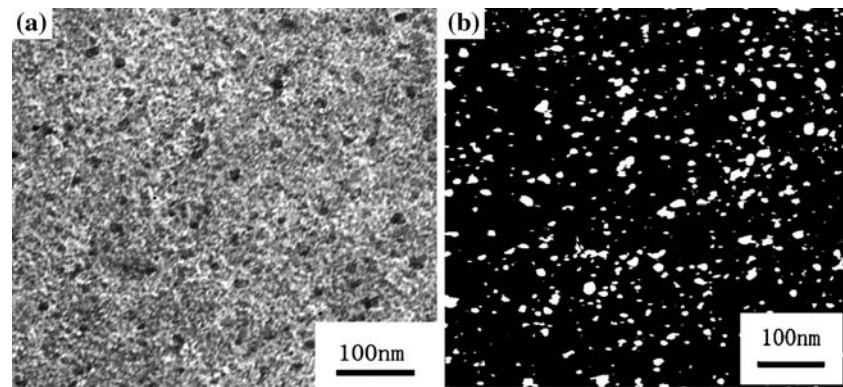


Fig. 7 The curves of resistivity $\rho(0)$, magnetic resistivity ρ_m , GMR vs. volume fraction at room temperature for FeCo–Cu granular films respectively

[19]. Meanwhile, it is clear that GMR effect first increases and then decreases with the volume fraction, reaching a maximum of about 0.7% at the volume fraction of 31%, which is very close to the GMR value of Ge [20]. By comparison, GMR effect has the same changing tendency as ρ_m , indicating that magnetic resistivity ρ_m is directly responsible for the GMR effect.

Combining the GMR effect of films with the average size of the same films, we can obtain the relationship between average granule size and GMR effect, as shown in Fig. 8. From Fig. 8, it is clear that GMR effect increases first and then decreases with increasing the average granule size, reaching a maximum at a certain middle granule size, which is in agreement with theory [21] and other experiments [22]. This behavior can be explained by the following physical viewpoints. On the one hand, the surface-to-volume ratio of the granules increases with

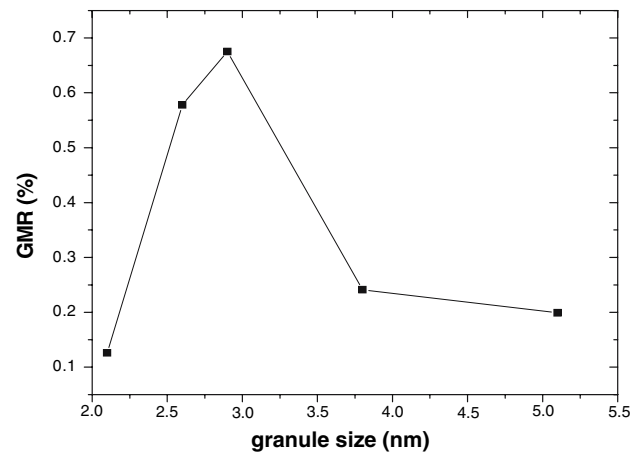


Fig. 8 Dependence of GMR on the granule size for FeCo–Cu films. The solid squares are experimental points and the solid lines are guides to the eyes

decreasing granule size, giving rise to the enhancement of the spin-dependent interface scattering and then GMR effect. On the other hand, the currents pass by granules easily when the granule size is smaller than the mean free path of electrons, giving rise to the reduction of spin-dependent interface scattering and then GMR effect. The competition between these factors leads to a maximum of the GMR effect at the middle granule size.

As mentioned above, all three kinds of magnetic granules in granular films have different effects on the spin-dependent scattering related to GMR effect. When granule size is very small, most granules in FeCo–Cu film behave as superparamagnetic, leading to the fact that the fraction of superparamagnetic granules is largest among three kinds of magnetic granules, while the GMR effect becomes smaller, indicating that superparamagnetic granules do not predominate in GMR effect. With increasing granule size, most granules gradually become larger and form single domain granules or multi-domain granules, causing the decrease of the fraction of superparamagnetic granules and the increase of the fraction of single domain granules or

multi-domain granules, meanwhile, GMR effect enhances, indicating that single domain granules or multi-domain granules predominate in GMR effect. With further increasing the granule size, most granules grow to be multi-domain granules, however, the GMR effect drops rapidly, indicating that multi-domain granules do not predominate in GMR effect. Therefore, it can be concluded from above analysis that single domain granules play a key role in GMR effect, which can be confirmed by annealing experiments, as shown in Fig. 9. Figure 9 shows the curves of GMR effect vs. annealing temperature for granular films with various volume fractions, from which it can be found that for films with lower volume fraction (13%vol. FeCo), the GMR effect reaches a maximum at higher temperature (673 K). With increasing the volume fraction, the GMR effect reaches a maximum at relative lower temperature, such as for film with 25%vol. FeCo at 573 K and for film with 31%vol. FeCo at 473 K. When the volume fraction increases further, the GMR effect has almost no changes at first, and then decreases with increasing the annealing temperature. This can be explained by our phenomenological viewpoint that single domain granules play a key role in GMR effect. For films with low volume fraction, all the magnetic granules are so small as to almost behave as superparamagnetic and the fraction of single domain granules is very low, thus leading to low GMR effect. Only when the annealing temperature is very high, some granules can grow to be single domain ones and the fraction of single domain granules reaches a maximum, thus GMR effect reaches a peak value. While for films with middle volume fraction, some granules are single domain granules before annealing, giving rise to the fact that the fraction of single domain granules reaches a maximum at relative low annealing temperature. For films with high volume fraction, some granules are multi-domain ones before

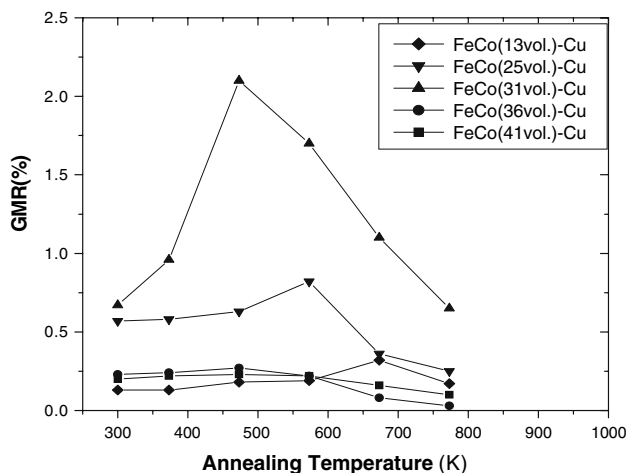


Fig. 9 The curves of GMR vs. annealing temperature for films with various volume fractions

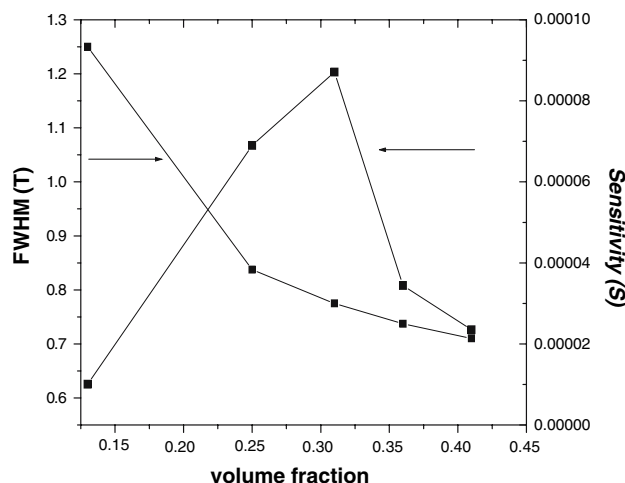


Fig. 10 The relationship of FWHM or sensitivity of TMR with the volume fraction

annealing. With increasing the annealing temperature, most granules further grow to be multi-domain ones, leading to very low fraction of single domain granules and then rapid decrease of GMR.

In addition, we investigate the dependence of the full width at half maximum (FWHM) and sensitivity of GMR effect, defined as $S = \text{GMR}/\text{FWHM}$ [23], on the volume fraction, respectively, as shown in Fig. 10. It is clear that with increasing the volume fraction, the FWHM decreases monotonically while the sensitivity reaches a maximum at about 31 vol.% FeCo corresponding to the maximum of the GMR effect. As discussed above that the fraction of three-kind granules changes with volume fraction, it implies that single domain and multi-domain granules are beneficial to the FWHM while only single domain granules is beneficial to sensitivity of GMR, which is attributed to the fact that superparamagnetic granules is very hard to rotate under applied field and multi-domain granules can decrease the GMR effect.

Conclusions

In summary, TEM observation showed that all as-deposited FeCo–Cu films consist of very fine FeCo granules uniformly dispersed in the Cu matrix and form fcc structure. Through fitting, the size distribution of FeCo in all as-deposited films satisfied a log-normal function. Meanwhile it was found that GMR effect of FeCo–Cu films changed non-monotonically with the volume fraction and reached a maximum of about 0.7% at the volume fraction of 31%, leading to the fact that GMR changed non-monotonically with granule size and reached a peak at a middle granule size. In addition, for films with lower volume fraction, the GMR reached a maximum at higher

annealing temperature while for films with high volume fraction the GMR reached a maximum at relative lower annealing temperature. Furthermore, the FWHM decreases monotonically while the sensitivity of GMR reaches a maximum at about 31 vol.% FeCo corresponding to the maximum of the GMR effect with increasing the volume fraction. All phenomena about GMR can be explained by the fact that single domain granule plays a key role in GMR.

Acknowledgments This work is financially supported by the Nature Science Foundation of Shandong Province under Grant No. 2005ZX11, Hi-Tech Research and development Program of China under Grant No.2004AA32G090 and National Nature Science Foundation of China under Grant No. 60571062.

References

1. Xiao JQ, Jiang JS, Chien CL (1992) *Phys Rev Lett* 68:3749
2. Berkowitz AE, Mitekell JR, Corey MJ et al (1992) *Phys Rev Lett* 68:3745
3. Gester A, Ounadjela K, Gregg JF et al (1997) *J Magn Magn Mater* 165:323
4. Milner A, Korenblit IYa, Gerber A (1999) *Phys Rev B* 60:14821
5. Chen SY, Yao YD, Wu JM (2006) *J Magn Magn Mater* 304:e37
6. Kim J-G, Ha J-G (2006) *Mater Chem Phys* 96:307
7. Cullity BD (1972) *Introduce to magnetic materials*. Addison-Wesley, London, p 383
8. Wang H, Li WQ, Wong SP et al (2002) *Mater Character* 48:153
9. Zhang S (1992) *Appl Phys Lett* 61:1855
10. Honda S, Nawate M, Tanaka M et al (1997) *J Appl Phys* 82:764
11. Sang H, Jiang ZS, Du YW (1995) *J Magn Magn Mater* 140/144:589
12. Gu RY, Sheng L, Xing DY et al (1996) *Phys Rev B* 53:11685
13. Xu C, Li Z-Y (1999) *Phys Lett A* 258:401
14. Hütten A, Bernardi J, Nelson C et al (1995) *Phys Solidi (A)* 150:171
15. Wang CZ, Guo ZH, Rong YH, Hsu TY (2004) *Phys Lett A* 329:236
16. Parent F, Tuailon J, Stern LB et al (1997) *Phys Rev B* 55:3683
17. Peng C, Dai D (1994) *J Appl Phys* 76:2986
18. Chien CL (1991) *J Appl Phys* 69:5267
19. Xiao JQ, Samuel Jiang J, Chien CL (1993) *IEEE Trans Mag* 29:2688
20. Ge S-H, Zhang Z-Z, Lu Y-Y et al (1997) *Thin Solid Films* 33:311
21. Zhang S, Levy PM (1993) *J Appl Phys* 73:5315
22. Wang W, Zhu F, Weng J et al (1998) *Appl Phys Lett* 72:1118
23. Hylton TL, Coffey KR, Parker MA et al (1993) *Science* 261:1021